Journal of the Optical Society of Korea
Vol. 13, No. 1, March 2009, pp. 65-74

DOI: 10.3807/JOSK.2009.13.1.065

Parametric Studies of Pulsed Laser Deposition of Indium Tin Oxide and Ultra-thin Diamond-like Carbon for Organic Light-emitting Devices

Teck-Yong Tou*, Thian-Khok Yong, Seong-Shan Yap, Ren-Bin Yang, Wee-Ong Siew, and Ho-Kwang Yow

Faculty of Engineering, Multimedia University, Cyberjaya, 63100 Selangor, Malaysia

(Received December 16, 2008 : revised February 4, 2009 : accepted February 6, 2009)

Device quality indium tin oxide (ITO) films are deposited on glass substrates and ultra-thin diamond-like carbon films are deposited as a buffer layer on ITO by a pulsed Nd:YAG laser at 355 nm and 532 nm wavelength. ITO films deposited at room temperature are largely amorphous although their optical transmittances in the visible range are > 90%. The resistivity of their amorphous ITO films is too high to enable an efficient organic light-emitting device (OLED), in contrast to that deposited by a KrF laser. Substrate heating at 200℃ with laser wavelength of 355 nm, the ITO film resistivity decreases by almost an order of magnitude to 2×10^{-4} Ω cm while its optical transmittance is maintained at > 90%. The thermally induced crystallization of ITO has a preferred <111> directional orientation texture which largely accounts for the lowering of film resistivity. The background gas and deposition distance, that between the ITO target and the glass substrate, influence the thin-film microstructures. The optical and electrical properties are compared to published results using other nanosecond lasers and other fluence, as well as the use of ultra fast lasers.

Molecularly doped, single-layer OLEDs of ITO/(PVK+TPD+Alq_3)/Al which are fabricated using pulsed-laser deposited ITO samples are compared to those fabricated using the commercial ITO. Effects such as surface texture and roughness of ITO and the insertion of DLC as a buffer layer into ITO/DLC/(PVK+TPD+Alq_3)/Al devices are investigated. The effects of DLC-on-ITO on OLED improvement such as better turn-on voltage and brightness are explained by a possible reduction of energy barrier to the hole injection from ITO into the light-emitting layer.

Keywords : Indium tin oxide, Pulsed Nd:YAG laser, Background gases, OLED

OCIS codes : (250.3680) Light-emitting polymers; (310.1860) Deposition and fabrication; (310.3849) Materials and process characterization ; (310.7005) Transparent conductive coatings

I. INTRODUCTION

A thin coating of indium tin oxide (ITO) [1] on glass or plastic substrates can be used as the transparent conducting electrode for flat-panel displays and acts as the hole-injection anode for organic light emitting devices (OLED) and organic solar cells. Common deposition methods include magnetron sputtering [2], spray pyrolysis [3], electron beam evaporation [4] and pulsed laser deposition (PLD) [5-14]. PLD of ITO using a KrF excimer laser by Kim et al. [6] reported a low resistivity of 2×10^{-4} Ωcm and an optical transmittance of 92% in the visible range. The ITO-coated glass was used successfully for OLED in which the performance was comparable to that of those fabricated using the commercial ITO. ITO has also been deposited using pulsed Nd:YAG laser at 355 nm [11-14] with a resistivity of about 1×10^{-4} Ωcm on heated glass and the optical transmittance was above 90%.

Ultrathin diamond-like carbon (DLC) film has been shown to influence the electrical characteristics, brightness and/or stability of OLEDs. For example, Lmimouni et al. [15] obtained two orders of magnitude increase in the injection-current of the polymer-based light emitting

*Corresponding author: tytou@mmu.edu.my

diodes, namely the ITO/P_3OT/DLC/Al and ITO/DLC/P_3OT/Al devices but the effects on their brightness were not reported in the article. Han et al. [16] obtained two orders of magnitude increase in the current in ITO/PEDOT:PSS/MEH-PPV/DLC/Al device using 1.5 nm DLC, but the OLED brightness decreased significantly. Choi et al. [17] showed that DLC acted as a diffusion barrier to prevent indium-ion contamination which improved the operation lifetime of OLED. Ultrathin DLC of 0.3-0.5 nm were also reported [18] to improve the brightness and lifetime of ITO/DLC/PEDOT/PPV/Ca/Ag. The improvement in OLED as a result of depositing DLC on ITO was explained in term of improved electron-hole charge balance in the light-emitting layer [17, 18].

We have found that a 1.5 nm DLC-on-ITO stabilized the dielectric breakdown of ITO/(PS+Alq_3+TPD)/Al device, due to weak electrical insulation of the light-emitting layer, which enabled the device operation to reach its maximum voltage [19]. This work was extended with ITO deposition on a glass substrate followed by DLC coating on ITO as a buffer layer with the aim of improving the electron-hole balance for OLED operation. In particular, the bulk and surface properties of ITO were optimized, compared with those deposited using KrF and intense fs lasers. Both ITO and DLC were deposited using a pulsed Nd:YAG laser with a third-harmonic output at 355 nm. Effects of DLC-on-ITO on the electrical characteristics and brightness investigated for in ITO/DLC/(PVK+Alq_3+TPD)/Al device, where PVK stands for poly-(N-vinylcarbazole) which was used as the polymer host. Co-doped with the hole-transport TPD or N,N'-diphenyl-N,N'-bis(3-methylphenyl)-1,1'-biphenyl-4,4'-diamine, and the electron-transport Alq_3 or tris-(8-hydroxyquinoline) -aluminium, the PVK layer would function as the light-emitting layer under the influence of externally applied voltage.

II. EXPERIMENTAL

2.1 Deposition and characterization of ITO and DLC

ITO films were grown on glass substrates using a Q-switched Nd:YAG pulsed laser (EKSPLA, NL301) output at 355 nm. The basic setup for pulsed Nd:YAG laser deposition of ITO films was reported previously [14]. The ablation target was a disk of 50-mm diameter and 6-mm thickness of sintered ITO ceramic (99.99 % purity), 90 wt% In_2O_3 and 10 wt% SnO_2 (Target Materials, Inc., USA). The focused laser beam was scanned over the target by an x-y motorized mirror with the glass substrate placed at 5 to 12 cm distance away, in the perpendicularly opposite position. The deposition chamber was evacuated to about 7×10^{-4} Pa and a background gas was introduced at a constant flow to maintain the desirable working pressure. The background gas was normally oxygen, but argon, nitrogen and helium were tried. The deposition rate was estimated to be 0.5 nm/second, or 0.05 nm/shot.

The deposited ITO was usually 200 nm thick, as measured by stylus profilometer (Perthometer S2, Mahr) and Zygo optical interferometer. The electrical resistivity of the ITO films was measured by using both the four-point probe technique and the van der Pauw Hall Effect technique (Hall-effect, Lake Shore Model 7507 HMS with EM7). The optical transmittance was obtained from the UV-Vis-NIR spectrophotometer, consisting of a deuterium-halogen light source (AvaLight-DHc, Avantes) and an optical multi channel analyzer (Ocean Optics) with spectral range between 200-850 nm. The surface roughness of ITO was determined by the atomic force microscope (AFM; Digital Instrument D5000), while the amorphous-to-polycrystalline transition in the ITO film microstructures was investigated by the XRD.

DLC film was deposited by Nd-YAG laser ablation of pyrolytic graphite (PG) target (99.999% purity, Kurt J. Lesker) at 45° incident angle in 10^{-6} Torr vacuum. Laser wavelength of 355 nm and 1064 nm with 1 Hz repetition rate and fixed fluences of ~12 J/cm^2 were used to produce two types of DLC films; DLC_{UV} and DLC_{IR}. The laser beam, focused to a 1 mm spot diameter was rastered over a 6.5 mm × 6.5 mm area on a graphite target by using an x-y motorized scanning mirror at a rate of 50 Hz. The substrates were placed at 12 cm from the target and the growth rate of DLC was ~0.02 nm per shot. DLC films are analyzed by using a Raman Spectrometer (Renishaw-2000), equipped with an argon laser with excitation λ = 514 nm.

2.2 OLED devices fabrication and characterizations

OLEDs were fabricated inside a nitrogen-filled glove box in a class-100 clean room. As mentioned in the early section, the OLEDs consisted of PVK as the host material that was doped with Alq_3 and TPD, which were dissolved in chloroform at 10 mg/ml of concentration. The ITO samples were patterned into vertical strips by wet etching using dilute aquaregia solution (HNO_3 (69%):HCl (37%):H_2O of 1:3:4). A 65-75 nm thick layer of (PVK+TPD+Alq_3) mixture was spin-coated on the ITO film. Horizontal strips of 50 nm thick aluminium cathode were then evaporated on the doped-PVK layer at 5×10^{-4} Pa of vacuum. The light-emitting area of OLED was about 0.075 cm^2, as defined by the overlapping area between the orthogonal strips of ITO and Al. Throughout this work, control samples of OLED were fabricated at the same time using commercial ITO-on-glass by the sputtering technique (sheet resistance ~ 28 Ω/sq, 70-nm-thick, transparency > 90 %).

DLC was coated either on the ITO anode or on the polymer layer to result in the device structure of Al/TPD-Alq_3 doped PVK/DLC/ITO or Al/DLC/TPD-Alq_3 doped PVK/ITO. A shadow mask was used to pattern

the ITO or polymer layer for selective area deposition of DLC film of 1 nm. The ITO-coated substrate was placed at 12 cm from the graphite target, and the deposition rate was 0.025 nm/shot. A high laser fluence of 12.5 J/cm^2, or laser power of 2×10^9 W/cm^2, was necessary to ablate a graphite target in order to achieve high sp^3 content. Visible Raman spectra from a 50-nm thick DLC indicated that the sp^3 content was probably 50% [19]. For DLC-coated-ITO, the speed of the spin-coater was reduced by half in order to obtain the same thickness of (PVK+TPD+Alq$_3$) layer.

The current–voltage (*I-V*) characteristic of the OLED was measured using the source-meter (Keithley 238 *I-V*) and controlled by the Interactive Characterisation Software (Metrics Technology Inc., USA). The electroluminescence (EL) intensity or brightness of the OLEDs was measured with an optical power meter (Oriel Instruments, model 70260) coupled to a silicon photodiode detector head (Oriel Instruments, model 70282).

III. RESULTS AND DISCUSSION

3.1 ITO film properties

(a) Electrical

Figure 1 shows the effects of substrate temperature on the electrical and optical properties. The resistivity is represented by a linear plot which shows a decrease of $(9.6\text{-}2.2)\times10^{-4}$ Ωcm with respect to temperature increase from 25-300℃. The inverse relationship is that the carrier density increases from 0.56 to 7.04×10^{20} cm^{-3}. The temperature effect has been reported to increase the surface diffusion of adsorbed particles on the ITO hence improving its film quality [20] due to the thermal induced crystallisation. The increase in carrier concentration may be due to an increase in the diffusion of Sn atoms from interstitial locations and grain boundaries into the In-cation sites. Since a Sn atom has a valency of 4 and In is trivalent, Sn atoms act as donors in ITO films.

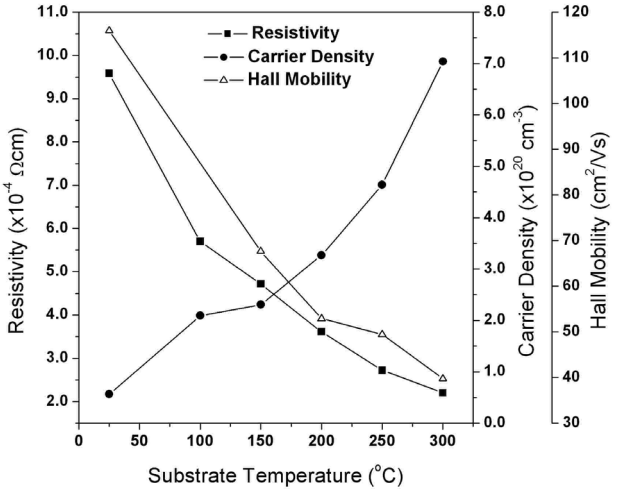

FIG. 1. Effect of substrate temperature on film resistivity, carrier density and Hall mobility. Deposition conditions: λ = 355-nm, fluence ~ 2.5 J/cm^2, target-to-substrate of 5 cm and O_2 pressure of about 5.3 Pa.

(b) Microstructures

The thermally induced crystallisation of the ITO film, as a result of substrate heating, is shown in Fig. 2a. Main XRD peaks of (222), (400), (440) and (622) indices appear and indicate the cubic In_2O_3 bixbyite structure. ITO films generally have a texture showing the preferred <111> directional orientation. These peaks split into two adjacent peaks, as reported previously by Yi et al. [21]. Also confirmed by results from Adurodija, et al. [22] for the ITO films prepared by a KrF excimer laser, the peak-splitting was attributed to the presence of two strained layers. These two effects could result from the

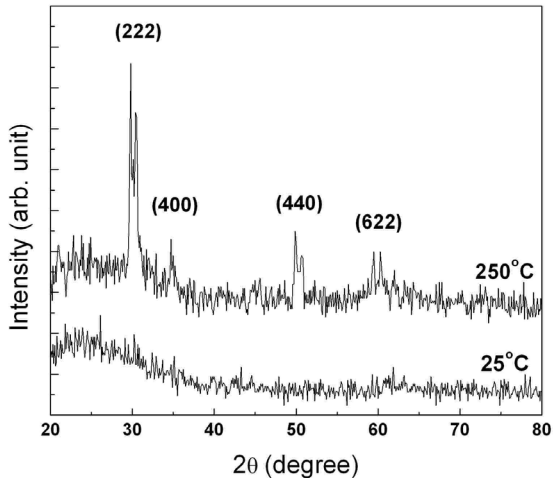

FIG. 2a. Effect of substrate temperature on microstructural changes.

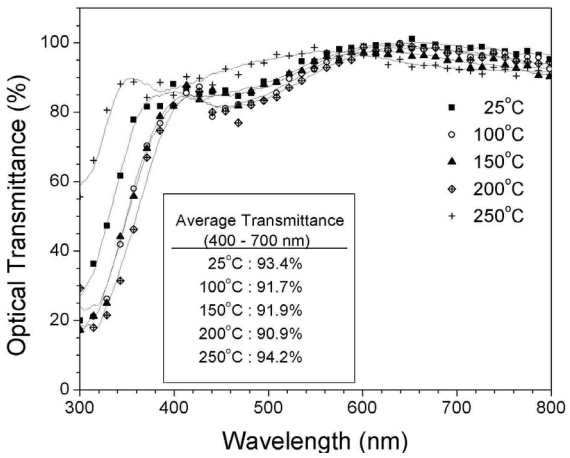

FIG. 2b. Effect of substrate temperature on optical transmittance.

stress that caused the changes in the XRD peak shifts and peak splitting. However, Yi et al. [21] attributed the peak-splitting to the thermal-assisted, solid-phase crystallisation which was responsible for the formation of the amorphous ITO layer on top of the substrate, and the vapour-phase crystallisation for the formation of polycrystalline ITO layer on top of the a-ITO layer.

(c) Optical Transmittance

At the optimum O_2 pressure, the optical transmittance in the visible region (400-700 nm) did not change appreciably with substrate heating, as shown in Fig. 2b. However, the absorption edge of the ITO film deposited at 250℃ shifts to a shorter wavelength, mainly due to the free-carrier absorption as result of increased carrier density. This is known as the Burstein-Moss shift [23] which correlates the shift to the increased filling up of the energy levels in the conduction band by electrons that are contributed by Sn atoms.

(d) Surface Morphology

Figure 3 shows the AFM images of our PLD-grown ITO films on 250℃ heated glass substrate at target-to-substrate distance (d_{TS}) of (a) 5 cm, (b) 8 cm and (c) 12 cm. The PLD-grown ITO film at 5 cm showed very smooth surface, as compared to the ITO films deposited at 8 cm and 12 cm. The root-mean-square roughness (R_{rms}) of these ITO films is 1.3 nm, 5 nm and 11 nm, respectively. The PLD-grown ITO film at 8 cm showed the columnar grain structures with an average size of 60 nm, whereas the ITO film deposited at 12 cm consisted of defected columns with wider voids between them. The energy of species impinging onto the substrate at 12 cm was lower than for those species impinging onto the substrate at 8 cm. As a result, the kinetics of atomic rearrangement was always lower for the substrate at 12 cm and thus the resulting ITO film surface had rougher morphology as compared to that at 5 cm and 8 cm.

(e) Comparison with KrF and Femto-second Laser Deposition

Table 1 compares the properties of ITO deposited on different substrates by KrF, Nd:YAG and femtosecond lasers. It is clear that there is still a lack of work being done on ITO deposition by using the intense fs laser, and effects of intensity and wavelength on the bulk and surface properties of ITO have not been investigated. It may be worthwhile to mention that surface modification of ITO at the nano-scale is expected to be easily carried out with relatively little damage by the fs laser, which may contribute to the improvement in the brightness and stability performance of OLEDs.

3.2 OLED performance

Figure 4 shows the brightness performance of different OLEDs as a function of the applied voltage for

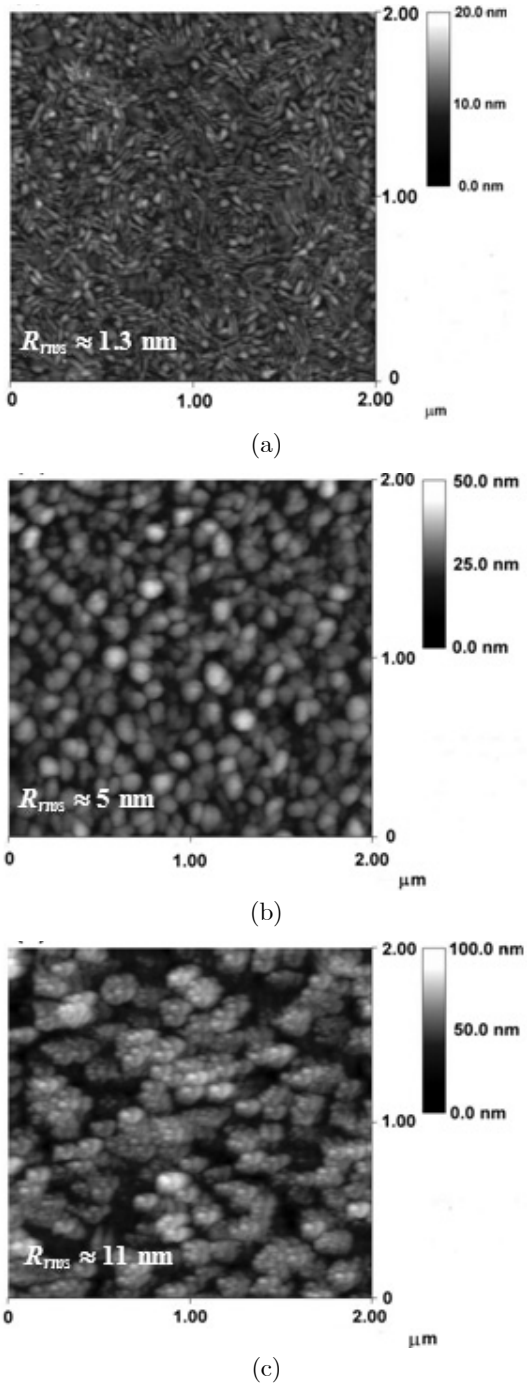

FIG. 3. AFM images (2μm × 2μm) of the PLD-grown ITO on 250℃ heated glass in 5.3 Pa of O_2 at target-to-substrate distances of (a) 5 cm, (b) 8 cm, and (c) 12 cm. The root-mean-square roughness (R_{rms}) of these ITO films is about 1.3 nm, 5 nm and 11 nm, respectively.

(i) OLED-1: commercial ITO; (ii) OLED-2: PLD-grown ITO/glass in Ar gas at 8 cm, (iii) OLED-3: PLD-grown ITO/glass in O_2 at 5 cm, (iv) OLED-4: PLD-grown ITO/glass in O_2 at 8 cm, and (iv) OLED-5: PLD-grown ITO/glass in O_2 at 12 cm. Compared to the commercial ITO, ITO deposited in O_2 at 5 cm which has a low sur-

TABLE 1. Comparison of the best properties of ITO films that were deposited on unheated and heated glass substrates by pulsed laser deposition for Nd:YAG laser (355nm), KrF laser (248nm) and femtosecond laser. (NA : not available)

Laser	Resistivity	Optical Transmittance	Surface Roughness
Nd:YAG: 4.7 ns, 355 nm	25℃: 1×10^{-3} cm 250℃: ~3×10^{-4} cm	92%	~ 3 nm
KrF: 30 ns, 248 nm	25℃: 4×10^{-4} cm 300℃: 2×10^{-4} cm	25℃: 85% 300℃: 92%	~ 0.5 nm
Nd:YAG: 250 fs, 527 nm	25℃: 1×10^{-3} cm 250℃: ~1×10^{-4} cm	NA	NA

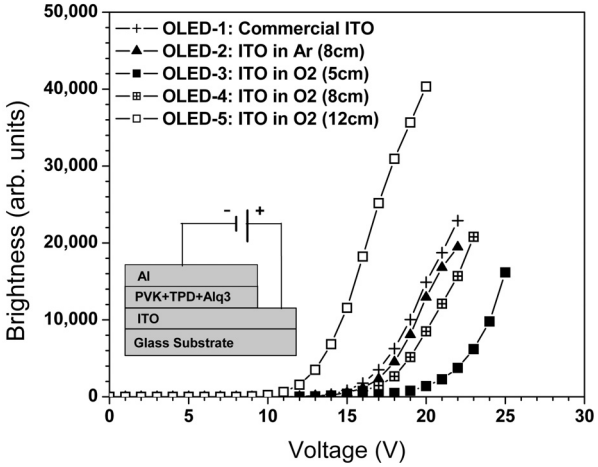

FIG. 4. The brightness as a function of operating voltage for ITO/PVK+TPD+Alq_3/Al OLEDs fabricated on different ITO in (i) commercial ITO, (ii) Ar gas, 8 cm, (iii) O_2 gas, 5 cm, (iv) O_2 gas, 8 cm, and (iv) O_2 gas, 12 cm.

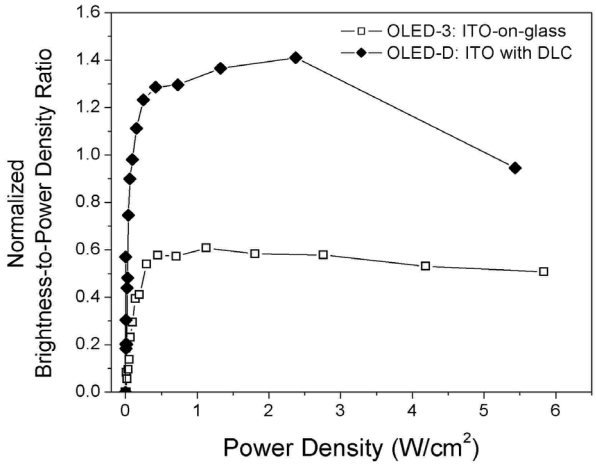

FIG. 5. Comparison of OLED normalized brightness-to -power density ratio characteristic and performance as a function of input power density, using PLD-grown ITO with and without DLC layer.

face roughness of about 1.3 nm, gives OLED with a relatively higher threshold voltage (+ 4.2 V) and a smaller operating voltage range (- 1.2 V), hence a lower maximum brightness (- 30 %). In addition, for ITO deposited in O_2 and at 12 cm, the OLED shows a remarkable improvement with a reduced threshold voltage (- 3.7 V), a higher rate of charge injection, a wider operating voltage range (+ 1.7 V) and hence an enhanced maximum brightness (+ 74 %). Wantz et al. [24] and Li et al. [25] reported that increasing the ITO surface roughness, by diluted aquaregia surface treatment, could greatly enhance their bi-layer OLED brightness although the lifetime was not investigated. They attributed the surface roughness effect to an increase of the anodic contact surface area and unevenness in enhancing the hole injection from the ITO layer into the hole transport layer. However, they did not observe a major shift in the threshold voltage. The main difference in the surface-roughness effect between these [24, 25] and our present work lies in a large threshold-voltage shift, which may be attributed to the difference of single-layer and double -layer OLEDs.

Compared to the OLED based on the commercial ITO, the differences in the threshold voltage and the operating voltage range for the OLEDs based on the ITO deposited in Ar and O_2 at 8 cm are less than 10 % while the maximum brightness is less by 13%. In a very recent article [26], the nano-structured surface of a metal-oxide film was shown to increase the charge injection in a multilayer polymer LED.

Figure 5 shows a plot of OLED brightness efficiency, which is normalised to the input power density and divided by the highest OLED brightness of the commercial ITO, for OLEDs based on ITO-on-glass and ITO that has been coated with an ultrathin DLC film. Even with our naked eyes, the effect of DLC-on-ITO observed was to remove most of the hot spots in OLED during initial stage of operation.

3.3 Effect of DLC

3.3.1 DLC properties

The Raman spectra of DLC films deposited by the 355-nm laser (DLC_{UV}) and 1064 nm laser (DLC_{IR}) are shown in Fig. 6. Each spectrum can be deconvoluted into 2 curves, known as the disorder D peak and the G peak. According to the Tunistra Koenig relation for

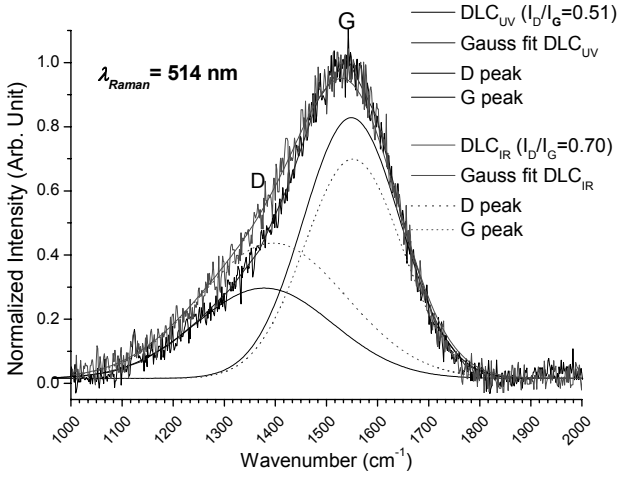

FIG. 6. Raman spectra of DLC films deposited by using 355 nm and 1064 nm laser.

amorphous carbon, the intensity ratios of the two fitted Gaussian peaks, I_D/I_G is proportional to L_a, which is the cluster diameter [27]. While the G peak of both films varied very little, the more prominent D peak in the 1064 nm laser deposited film signified graphite clustering and hence is slightly higher in sp^2 hybridization. The 355 nm laser deposited film is also high in resistivity; 4 orders higher than those deposited by 1064 nm laser. The intrinsic average roughness R_a of DLC films (20 nm), measured on silicon substrates were ~0.20 nm for DLC_{UV} and ~0.54 nm for DLC_{IR}. It has been reported that superior smoothness can be achieved independent of thickness such that AFM of 0.9 nm thick films remain 0.13 nm in roughness [28]. The dependence of DLC on deposition wavelength is consistent with the reports by others [29, 30]. At higher photon energy, lower penetration depth of shorter wavelength laser in the ablation of graphite results in higher ionized energetic species for subplantation growth of high sp^3 content DLC films [31].

3.3.2 OLED Performance

Light emissions were observed for a series of PVK-based devices with polymer thickness of 70-75 nm. This series consist of a standard device (ITO/polymer/Al), a device with DLC_{UV} (ITO/DLC_{UV}/polymer/Al), a device with DLC_{IR} (ITO/DLC_{IR}/polymer/Al) and a device with DLCUV deposited between the polymer layer and Al cathode (ITO/polymer/DLC_{UV}/Al). All of the devices were emitting in the green region with a peak wavelength at 520 nm as detected by the spectrometer, indicating that the luminescence was dominated by the Alq_3 compound and unaffected by the insertion of DLC. Figure 7 shows the current-voltage characteristics and brightness-voltage curve for all of the devices. The current-on voltages, $V_{I\text{-}on}$ for the devices were determined at 1 mA/cm^2, below which current fluctuation occurred

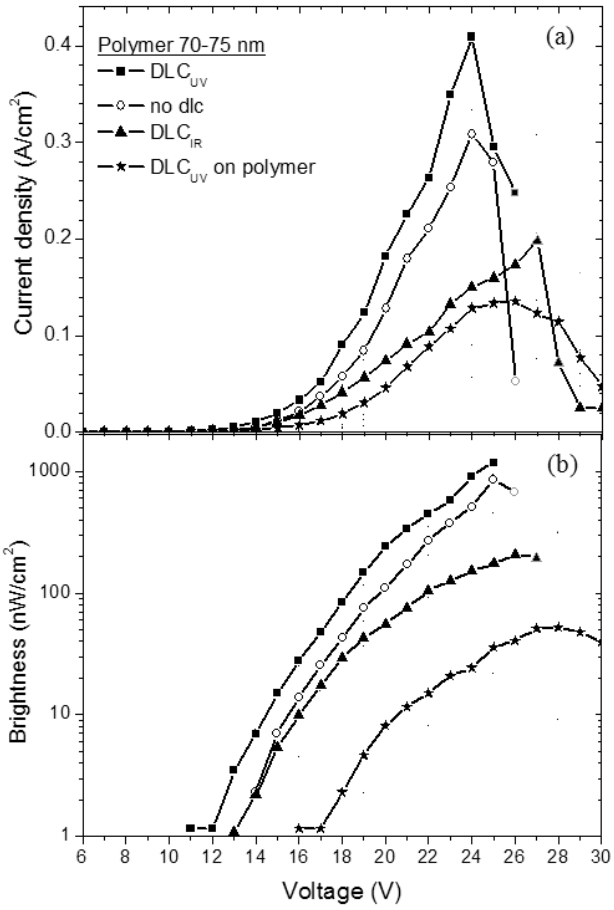

FIG. 7. Current density (a) and brightness (b) as a function voltage for OLED with and without DLC. The thickness of the polymer layers were 70-75 nm.

while the light-on-voltages, $V_{L\text{-}on}$ were obtained at threshold brightness of 1 nW/cm^2. Generally, maximum current injection (I_{max}) and brightness (L_{max}) for the devices with optimum thickness range decreased in the following order: ITO/DLC_{UV}/polymer/Al > ITO/polymer/Al > ITO/DLC_{IR}/polymer/Al > ITO/polymer/DLC_{UV}/Al.

The *I-V* characteristic and brightness of various OLEDs are summarized in Table 2. The device configuration of ITO/DLC_{UV}/polymer/Al has shown more rapid increase of current injection with VI-on of about 1.5 V less than a standard device. The maximum current density is 0.4 A/cm^2 at 24 V; after which the device failed and current dropped abruptly.

On the contrary, ITO/DLCIR/polymer/Al devices showed lower maximum current density and brightness than that of a standard device. The insertion of DLC, when positioned between polymer and Al layer, showed a detrimental effect for both thickness series where maximum current density was reduced by half (50%) of that for a control device sample. These devices show saturation and gradual decrease in current density before devices finally failed at higher voltage than standard

Table 2. Comparison of the ITO/PVK+TPD+Alq_3/Al OLED performances for ITO deposited in Ar and O_2, and that of the commercially available ITO. The deposition distance for O_2 (5, 8 and 12 cm) has a profound effect on the threshold or turn on voltage.

Sample	Type of ITO	Turn-on voltage at brightness of 1,000 a.u.	Brightness at voltage of 20 V
OLED-1	Commercial ITO	15.8 V	16,400 a.u.
OLED-2	Ar, 8cm	15.7 V	13,700 a.u.
OLED-3	O_2, 5 cm	19.6 V	1,330 a.u.
OLED-4	O_2, 8 cm	16.2 V	8,000 a.u.
OLED-5	O_2, 12 cm	11.8 V	46,700 a.u.

Table 3. The device characteristics of PVK based OLED with and without the DLC insertion for polymer thickness of 70-75 nm.

Device structure	$V_{\text{I-on}}$ (V)	$V_{\text{L-on}}$ (V)	$L_{\max}$ (nW/cm^2)	$I_{\max}$ (mA/cm^2)	Vmax (V)
ITO/polymer/Al	12.0	13.0	844	0.31	24
ITO/DLC_{UV}/polymer/Al	10.5	12.0	1185	0.41	24
ITO/DLC_{IR}/polymer/Al	12.0	13.0	195	0.20	27
ITO/polymer/ DLCUV/Al	12.0	17.0	36	0.14	25

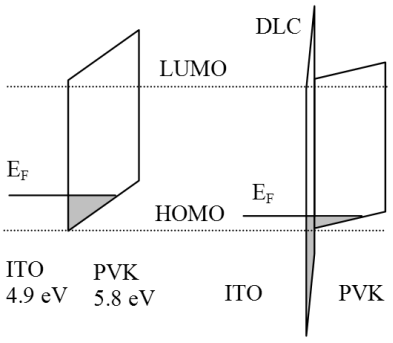

FIG. 8. The optimal effect of insertion of a DLC buffer between ITO anode and PVK, the barrier is indicated by the shaded area.

device or devices with DLC_{UV}. Besides brightness, devices light-on at different voltages. $V_{\text{L-on}}$ of 12 V are recorded for DLC_{UV} for devices of both polymer thicknesses while the standard device and ITO/DLC_{IR}/polymer/Al light-on at 13 V. DLC_{UV} -cathode samples show fairly high light on voltage at 17-18 V.

In contrast to the previous reports [14, 17], the improvement of surface roughness with DLC has minor effect in this study. The improved performance of insertion of high resistivity/sp^3 DLC_{UV} suggests the possibility of its role as insulating buffer for OLED, such as of LiF [32-35], metal oxide [36-39], SiO_2 [40], MgF_2 [41] and polymer [42]. Besides physically acting as interdiffusion barrier in high mobility materials, the mechanism for the enhancement by insulating buffers is generally explained by either the increase of probability of carrier tunneling with thin insulating layer or injection enhancement by low work function buffer. The latter requires low work function materials, which is appropriate for electrons only, while the tunneling process is applicable for most materials. It is also worthwhile mentioning that instead of tunneling, the opposite effect of hole-blocking by the buffer layer, although it reduced the current injection, can finally increase the device efficiency because of electron-hole balance for devices with MgF_2, SiO_2 and DLC [18, 41-43].

With higher current injection and brightness, the highly insulating DLC in this case is more reasonably explained as a potential barrier that allows tunneling of carriers. The positive effect of injection barrier reduction can be due to the potential drop across the buffer and/or shifting of the Fermi level at the interface as illustrated in Fig. 8 [44-46]. The primary requirement of such a buffer is that it should be sufficiently thin to enable tunneling and it should also be able to withstand the high electric field. In addition, factors like the resistivity and the relative position of the work function at the buffer-organic layer interface for both ITO anode side and metal cathode have been documented [44]. The effect of highly insulating DLC_{UV} as a buffer layer in our OLEDs is reflected in the lower $V_{\text{I-on}}$ and $V_{\text{L-on}}$. In addition, the hole transporting capability in PVK may assist in the OLED operation where hole injection and in this case, tunneling occurs directly into the PVK layer [47]. The internal barrier height (IBH) [44] where DLC was inserted, is thus 0.9 eV for ITO and PVK interface.

Devices with DLC_{IR} are inadequate for this process,

probably due to the relative lower resistivity at this thickness. For ITO/polymer/DLC$_{UV}$/Al, brightness enhancement was not obtained, in contrast to our previous report where polystyrene (PS) was used [19]. An increase in both $V_{I\text{-}on}$ and $V_{L\text{-}on}$ indicates that the potential drop across the device is too high; very thin DLC may be needed. In addition, PVK provides the hole transporting media and has been reported to be useful as electron blocking materials, and may even obstruct electron injection/tunneling.

IV. CONCLUSIONS

Optical transmittance and electrical properties of ITO deposited by a pulsed Nd:YAG laser were optimized by varying the deposition condition. These included the partial pressures of oxygen and argon as the background gases and the substrate-heating temperature, while the deposition distance influenced the surface morphology of ITO. These ITO properties influenced the turn-on voltage, current density and the maximum brightness of OLEDs. Literature search showed little work has been carried out using intense fs laser for the ITO deposition, and modifications of ITO surface properties were proposed using fs laser without causing physical damage.

The insertion of a 1.5-nm DLC in OLEDs might or might not improve their brightness. Deposited by UV laser wavelength at 355nm on the ITO, the DLC layer lowered the turn-on voltage, increased the current density and hence the OLED brightness. In contrast, the DLC layer deposited on ITO by the IR laser wavelength and also that deposited on the light-emitting polymer (before Al cathode) by the UV laser wavelength deteriorated the OLED performance in terms of current density and brightness. The OLED improvement by DLC deposited on ITO was explained by the reduction of energy barrier which facilitated the hole injection from ITO anode. The poor OLED performance as a result of DLC deposition on the light-emitting polymer layer was due to the suppression of electron injection from the aluminium cathode.

ACKNOWLEDGMENTS

This project is supported by the research grants from Malaysia Toray Science Foundation (MTSF) (project no: 140372) and Malaysia Ministry of Science, Technology and Innovation (MOSTI) (project no: 140356) and Shin -Etsu Handotai (S.E.H.) Malaysia Sdn. Bhd. for access to AFM measurements.

REFERENCES

1. H. L. Hartnagel, A. L. Dawar, A. K. Jain, and C. Jagadish, *Semiconducting Transparent Thin Films* (Institute of Physics Publishing, Bristol and Philadelphia, 1995).
2. L. Meng and M. P. dos Santos, "Properties of indium tin oxide (ITO) films prepared by r.f. reactive magnetron sputtering at different pressures," Thin Solid Films **303**, 151-155 (1997).
3. C. G. Choi, K. No, W. J. Lee, H. G. Kim, S. O. Jung, W. J. Lee, W. S. Kim, S. J. Kim, and C. Yoon, "Effects of oxygen partial pressure on the microstructure and electrical properties of indium tin oxide film prepared by d.c. magnetron sputtering," Thin Solid Films **258**, 274-278 (1995).
4. H. Bisht, H.-T. Eun, A. Mehrtens, and M. A. Aegerter, "Comparison of spray pyrolyzed FTO, ATO and ITO coatings for flat and bent glass substrates," Thin Solid Films **351**, 109-114 (1999).
5. J. P. Zheng and H. S. Kwok, "Low resistivity indium tin oxide films by pulsed laser deposition," Appl. Phys. Lett. **63**, 1-3 (1993).
6. H. Kim, C. M. Gilmore, A. Piqué, J. S. Horwitz, H. Mattoussi, H. Murata, Z. H. Kafafi, and D. B. Chrisey, "Electrical, optical, and structural properties of indium–tin–oxide thin films for organic light-emitting devices," J. Appl. Phys. **86**, 6451-6461 (1999).
7. H. Kim, J. S. Horwitz, G. P. Kushto, Z. H. Kafafi, and D. B. Chrisey, "Indium tin oxide thin films grown on flexible plastic substrates by pulsed-laser deposition for organic light-emitting diodes," Appl. Phys. Lett. **79**, 284 -286 (2001).
8. F. O. Adurodija, H. Izumi, T. Ishihara, H. Yoshioka, and M. Motoyama, "Highly conducting indium tin oxide (ITO) thin films deposited by pulsed laser ablation," Thin Solid Films **350**, 79-84 (1999).
9. H. Izumi, T. Ishihara, H. Yoshioka, and M. Motoyama, "Electrical properties of crystalline ITO films prepared at room temperature by pulsed laser deposition on plastic substrates," Thin Solid Films **411**, 32-35 (2002).
10. M. A. Morales-Paliza, M .B. Huang, and L. C. Feldman, "Nitrogen as background gas in pulsed-laser deposition growth of indium tin oxide films at room temperature," Thin Solid Films **429**, 220-224 (2003).
11. E. Holmelund, B. Thestrup, J. Schou, N. B. Larsen, M. M. Nielsen, E. Johnson, and S. Tougaard, "Capacitance –voltage characteristics of liquid crystal displays with periodic interdigital electrodes," Appl. Phys. A **74**, 147-149 (2002).
12. B. Thestrup, J. Schou, A. Nordskov, N. B. Larsen, "Electrical and optical properties of thin indium tin oxide films produced by pulsed laser ablation in oxygen or rare gas atmospheres," Appl. Surf. Sci. **142**, 248-252 (1999).
13. J. B. Choi, J. H. Kim, K. A. Jeon, and S. Y. Lee, "Properties of ITO films on glass fabricated by pulsed laser deposition," Mater. Sci. Eng. B **102**, 376-379 (2003).
14. T. K. Yong, S. S. Yap, G. Sáfrán, and T. Y. Tou, "Pulsed Nd: YAG laser depositions of ITO and DLC films

for OLED applications," Appl. Surf. Sci **253**, 4955 -4959 (2007).
15. K. Lminouni, C. Legrand, C. Dufour, and A. Chapoton, "Diamond-like carbon films as electron-injection layer in organic light emitting diodes," Appl. Phys. Lett. **78**, 2437 -2439 (2001).
16. D. W. Han, S. M. Jeong, S. J. Lee, N. C. Yang, and D. H. Suh, "Electron injection enhancement by diamond-like carbon film in organic electroluminescence devices," Thin Solid Films **420-421**, 190-194 (2002).
17. S. H. Choi, S. M. Jeong, W. H. Koo, S. J. Jo, H. K. Baik, S. J. Lee, K. M. Song, and D. W. Han, "Diamond-like carbon as a buffer layer in polymeric electroluminescent device," Thin Solid Films **483**, 351-357 (2005).
18. B. J. Chen, X. W. Sun, B. K. Tay, L. Ke, and S. J. Chua, "Improvement of efficiency and stability of polymer light -emitting devices by modifying indium tin oxide anode surface with ultrathin tetrahedral amorphous carbon film," Appl. Phys. Lett. **86**, 63506-1-3 (2005).
19. S. S. Yap, R. B. Yang, H. Y. Yow, and T. Y. Tou, "Enhanced reliability by diamond-like carbon in single-layer organic light emitting diodes," Electronic Letters **42**, 114-115 (2006).
20. R. B. H. Tahar, T. Ban, Y. Ohya, and Y. Takahashi, "Tin doped indium oxide thin films: electrical properties," J. Appl. Phys. **83**, 2631-2645 (1998).
21. C. H. Yi, Y. Y. Shigesato, I. Yasuui, and S. Takaki, "Microstructure of low-resistivity tin-doped indium oxide films deposited at 150 ~ 200℃," Jpn. J. Appl. Phys. **34**, L244-L247 (1995).
22. F. O. Adurodija, H. Izumi, T. Ishihara, H. Yoshioka, and M. Motoyama, "Effects of stress on the structure of indium-tin-oxide thin films grown by pulsed laser deposition," J. Mater. Sci.: Mater. Electron. **12**, 57-61 (2001).
23. E. Burstein, "Anomalous optical absorption limit in InSb," Phys. Rev. **93**, 632-633 (1954).
24. G. Wantz, L.Hirsch, N. Huby, L.Vignau, J. F. Silvain, A. S. Barriére, and J. P. Parneix, "Correlation between the indium tin oxide morphology and the performances of polymer light-emitting diodes," Thin Solid Films **485**, 247-251 (2005).
25. F. Li, H. Tang, J. Shinar, O. Resto, and S. Z. Weisz, "Effects of aquaregia treatment of indium–tin–oxide substrates on the behavior of double layered organic light-emitting diodes," Appl. Phys. Lett. **70**, 2741-2743 (1997).
26. S. A. Haque, S. Koops, N. Tokmoldin, J. R. Durrant, J. Huang, D. D. C. Bradley, and E. Palomares, "A multilayered polymer light-emitting diode using a nanocrystalline metal-oxide film as a charge-injection electrode," Adv. Mater. **19**, 683-687 (2007).
27. A. C. Ferrari and J. Robertson, "Resonant raman spectroscopy of disordered, amorphous, and diamond-like carbon," Phys. Rev. B **64**, 075414-13 (2001).
28. C. Casiraghi, A. C. Ferrari, R. Ohr, A. J. Flewitt, D. P. Chu, and J. Robertson, "Dynamic roughening of tetrahedral amorphous carbon," Phys. Rev. Lett. **91**, 226104 -1-4 (2003).
29. K. Yamamoto, Y. Koga, S. Fujiwara, F. Kokai, and R. B. Heimann, "Dependence of the sp^3 bond fraction on the laser wavelength in thin carbon films prepared by pulsed laser deposition," Appl. Phys. A: Mater. **66**, 115-117 (1998).
30. T. Yoshitake, T. Nishiyama, H. Aoki, K. Suizu, K. Takahashi, and K. Nagayama, "The effects of substrate temperature and laser wavelength on the formation of carbon thin films by pulsed laser deposition," Diamond Relat. Mater. **8**, 463-465 (1999).
31. J. Robertson, "Mechanism of sp^3 bond formation in the growth of diamond-like carbon," Diamond Relat. Mater. **14**, 942-948 (2005).
32. Y. Zhao, S. Y. Liu, and J. Y. Hou, "Effect of LiF buffer layer on the performance of organic electroluminescent devices," Thin Solid Films **397**, 208-210 (2001).
33. J. Xiao, Z. B. Deng, C. J. Liang, D. H. Xu, Y. Xu, and D. Guo, "Effect of LiF buffer layer on the performance of organic electroluminescent devices," Physica E **28**, 323-327 (2005).
34. H. J. Li, R. H. Zhu, X. Y. Li, Z. J. Wang, and B. C. Yang, "Determination of the optimal thickness of inserted LiF in bilayer organic light-emitting devices," Solid State Commun. **144**, 445-447 (2007).
35. K. Han, Y. Yi, W. J. Song, S. W. Cho, P. E. Jeon, H. Lee, C. N. Whang, and K. Jeong, "Dual enhancing properties of LiF with varying positions inside organic light -emitting devices," Org. Electron. **9**, 30-38 (2008).
36. H. You, Y. F. Dai, Z. Q. Zhang, and D. G. Ma, "Improved performances of organic light-emitting diodes with metal oxide as anode buffer," J. Appl. Phys. **101**, 026105-1-3 (2007).
37. H. W. Choi, S. Y. Kim, W. K. Kim, K. Hong, and J. L. Lee, "Effect of magnesium oxide buffer layer on performance of inverted top-emitting organic light-emitting diodes," J. Appl. Phys. **100**, 064106-1-6 (2006).
38. H. W. Choi, S. Y. Kim, W. K. Kim, and J. L. Lee, "Enhancement of electron injection in inverted top-emitting organic light-emitting diodes using an insulating magnesium oxide buffer layer," Appl. Phys. Lett. **87**, 082102-1-3 (2005).
39. S. T. Zhang, Y. C. Zhou, J. M. Zhao, Y. Q. Zhan, Z. J. Wang, Y. Wu, X. M. Ding, and X. Y. Hou, "Role of hole playing in improving performance of organic light -emitting devices with an Al_2O_3 layer inserted at the cathode-organic interface," Appl. Phys. Lett. **89**, 043502 -1-3 (2006).
40. Z. B. Deng, X. M. Ding, S. T. Lee, and W. A. Gambling, "Enhanced brightness and efficiency in organic electroluminescent devices using SiO_2 buffer layers," Appl. Phys. Lett. **74**, 2227-2229 (1999).
41. B. J. Chen and X. W. Sun, "The role of MgF_2 buffer layer in tris-(8-hydroxyquinoline)aluminium-based organic light -emitting devices with Mg:Ag cathode," Semicon. Sci. Tech. **20**, 801-804 (2005).
42. Z. X. Wu, L. D. Wang, H. F. Wang, Y. D. Gao, and Y. Qiu, "Charge tunneling injection through a thin teflon film between the electrodes and organic semiconductor layer: relation to morphology of the teflon film," Phys. Rev. B. **74**, 165307-1-7 (2006).
43. B. J. Chen, X. W. Sun, B. K. Tay, L. Ke, and S. J. Chua, "Improvement of efficiency and stability of polymer light -emitting devices by modifying indium tin oxide anode surface with ultrathin tetrahedral amorphous carbon film," Appl. Phys. Lett. **86**, 063506-1-3 (2005).
44. S. T. Zhang, X. M. Ding, J. M. Zhao, H. Z. Shi, J. He,

Z. H. Xiong, H. J. Ding, E. G. Obbard, Y. Q. Zhan, W. Huang, and X. Y. Hou, "Buffer-layer-induced barrier reduction: role of tunneling in organic light-emitting devices," Appl. Phys. Lett. **84**, 425-427 (2004).

45. X. J. Wang, J. M. Zhao, Y. C. Zhou, X. Z. Wang, S. T. Zhang, Y. Q. Zhan, Z. Xu, H. J. Ding, G. Y. Zhong, H. Z. Shi, Z. H. Xiong, Y. Liu, Z. J. Wang, E. G. Obbard, X. M. Ding, W. Huang, and X. Y. Hou, "Enhancement of electron injection in organic light-emitting devices using an Ag/LiF cathode," J. Appl. Phys. **95**, 3828-3830 (2004).
46. J. M. Zhao, Y. Q. Zhan, S. T. Zhang, X. J. Wang, Y. C. Zhou, Y. Wu, Z. J. Wang, X. M. Ding, and X. Y. Hou, "Mechanisms of injection enhancement in organic light-emitting diodes through insulating buffer," Appl. Phys. Lett. **84**, 5377-5379 (2004).
47. M. Goes, J. W. Verhoeven, H. Hofstraat, and K. Brunner, "OLED and PLED devices employing electrogenerated, intramolecular charge-transfer fluorescence," Chem. Phys. Chem. **4**, 349-358 (2003).